Steel and Composite Structures, *Vol. 26*, *No. 5* (*2018*) *607-620*
DOI: https://doi.org/10.12989/scs.2018.26.5.607

Free vibration of deep curved FG nano-beam based on modified couple stress theory

O. Rahmani *, S.A.H. Hosseini, I. Ghoytasi and H. Golmohammadi

Smart Structures and New Advanced Materials Laboratory, *Department of Mechanical Engineering*, *University of Zanjan*, *Zanjan*, *Iran*

(*Received June 05*, *2017*, *Revised December 4*, *2017*, *Accepted December 22*, *2017*)

Abstract. Vibration analysis of deep curved FG nano-beam has been carried out based on modified couple stress theory. Material properties of curved Timoshenko beam are assumed to be functionally graded in radial direction. Governing equations of motion and related boundary conditions have been obtained via Hamilton's principle. In a parametric study, influence of length scale parameter, aspect ratio, gradient index, opening angle, mode number and interactive influences of these parameters on natural frequency of the beam, have been investigated. It was found that, considering geometrical deepness term leads to an increase in sensitivity of natural frequency about variation of aforementioned parameters.

Keywords: deep curved nano beam; Timoshenko beam model; functionally graded material; modified couple stress; vibration analysis

1. Introduction

Papers, studies and experiments show that size-dependent behavior is an inseparable characteristic of every kind of structures in micron and submicron scale. Thus for studying micro- and sub micro-structures practical theories should be used to capture such size effect.

Several higher order and non-local elasticity theories have been used to develop nano structure-dependent beam models (Jandaghian and Rahmani 2015, Hosseini and Rahmani 2016b) but in this study couple stress theory is introduced emphatically and other theories are introduced just for discovering the history.

Chong and Lam (1999) showed that size-dependent effect phenomenon is not only appertaining to special materials such as metals, but also it is detected in some kinds of polymers. By micro-bending tests of beams made of epoxy polymers, McFarland and Colton (2005) detected a considerable difference between the stiffness values predicted by the classical beam theory and the stiffness values obtained during a bending test of polypropylene micro-cantilever.

After that a model has been developed for the bending of Euler-Bernoulli beam subjected to a point load by Park and Gao (2006) using a modified couple stress theory proposed by Yang *et al*. (2002) which contains only one material length scale parameter. They employed a variational formulation based on the principle of minimum total potential energy (Park and Gao 2008b).

Nowadays scientists and engineers usually use couple stress theory (Park and Gao 2008a, Shafiei *et al*. 2015).

Ma *et al*. (2008) developed a Timoshenko beam model to study static deformation and free-vibration frequencies such beam based on a modified couple stress theory, Poisson's effect and Hamilton's principle which does not only incorporate bending and axial deformations like the classical Timoshenko beam theory but also a material length scale parameter that it could capture the size effect. This model can recover the classical Timoshenko beam model when the material length scale parameter and Poisson's ratio are both set to be zero.

Linear solutions about analysis of beams based on couple stress theory, which mentioned formerly, are not able to study nonlinear conditions such above beam researches. Xia *et al*. (2010) presented a size dependent nonlinear Euler-Bernoulli beam model based on modified couple stress theory in which the nonlinear size dependent static bending, buckling and the free vibration of beams were studied. Asghari *et al*. (2010) developed a nonlinear size dependent Timoshenko beam model based on the modified couple stress theory which is a non-classical continuum theory capable of capturing the size effect.

After straight beam models at last it was curved beams turn to be investigated (Ebrahimi and Daman 2016, 2017, Hosseini and Rahmani 2016a Rahmani *et al*. 2016). In 2011, Liu and Reddy (2011) developed a non-local Timoshenko curved beam model based on a modified couple stress theory and Hamilton's principle which contains only one material length scale parameter capable of capturing the size effect. Poisson's effect is incorporated in the model as well. This model will recover the classical model if the material length scale parameter and Poisson's ratio are both taken to be zero and it will recover straight beam model if the radius of curvature of the beam is set to infinity. In addition, the non-local Euler-Bernoulli curved beam model can be realized if the normal cross section assumption is restated.

*Corresponding author, Associate Professor,
E-mail: omid.rahmani@znu.ac.ir

ISSN: 1229-9367 (Print), 1598-6233 (Online)

Tsiatas (2009) introduced a new Kirchhoff plate model based on a modified couple stress theory. Jomehzadeh *et al*. (2011) investigated size dependent vibration analysis of micro plates based on a modified couple stress theory. Ma (2011) developed a nonclassical Mindlin plate model using a modified couple stress theory involving a material length scale parameter, which can capture size effect. It can be reduced to Mindlin plate model based on classical elasticity theory when the material length scale parameter is set to be zero.

By developing different size dependent nano structural models based on various theories even FGMs put under investigation by researchers.

Shariat and Eslami (2007) investigated buckling of thick FG plates under mechanical and thermal loads. Roque *et al*. (2007) developed a radial basis function for the free vibration analysis of functionally graded plates using a refined theory. Darabi *et al*. (2008) developed a nonlinear analysis of dynamic stability for functionally graded cylindrical shells under periodic axial loading. Lanhe *et al*. (2007) studied dynamic stability analysis of FG plates by the moving least squares differential quadrature method

Simsek *et al*. (2013) investigated the bending behavior of FG Timoshenko micro beams based on modified couple stress theory. Simsek and Reddy (2013) examined static bending and free vibration of functionally graded micro scale Timoshenko beams based on a modified couple stress theory. Their results proved that neglecting Poisson's ratio changes the results significantly. Arbind and Reddy (2013) investigated a micro structure nonlinear third-order FG beam based on modified couple stress and a power-law variation of the material and the Von Karman nonlinear strains using Hamilton's principle. Akgoz and Civalek (2013) investigated free vibration analysis of axially functionally graded tapered Euler-Bernoulli micro beams based on the modified couple stress theory. Thai and Choi (2013) investigated size dependent FG Kirchhoff and Mindlin micro plate models and analyzed their static bending, buckling and free vibration by using a modified couple stress-based theory. To avoid the use of the shear correction factor Salamat-talab *et al*. (2012) and Nateghi *et al*. (2012) utilized modified couple stress theory to study static and dynamic analysis of FG micro beam and size dependent buckling analysis of functionally graded micro beams based on third-order shear deformation theory, respectively. Mohammad-Abadi and Daneshmehr (2014) studied buckling analysis of Euler-Bernoulli, Timoshenko and Reddy beams based on modified couple stress theory. To examine the effect of boundary conditions, three kinds of boundary conditions containing hinged-hinged, clamped-hinged and clamped-clamped are considered. Governing equations and boundary conditions are derived, using principle of minimum potential energy and generalized differential quadrature method is employed to solve the governing differential equations.

All of the beams are partially curved in practice, even with small angles (Nie and Zhong 2012, Zand 2012, Fereidoon *et al*. 2015). However, in order to facilitate calculations and mathematical treatments, in previous researches straight beam theories have been utilized, while curved beam theories are more generalized than those of straight beams because by setting radius of curvature to infinity, utilized model degenerates to straight beam model. According to the previously conducted studies and available results, a gap is found in the open literature that is lack of a sufficient study on vibration characteristics of a deep curved FG nano beam based on MCST. The aim of this work is to fill the gap.

The rest of the paper is organized as follows. In Section 2 formulation of a deep curved FG nano beam is derived based on modified couple stress and Timoshenko beam theories, using Hamilton's principle. Then in Section 3 Navier's solution method is employed in order to solve the obtained differential equation. In Section 4 obtained numerical results are discussed and influences of dimensionless length scale parameter, aspect ratio, gradient index, arc angle, mode number and their interactive influences on natural frequency are investigated and finally in order to validation, the presented results are compared with those of a previous work. The paper concludes in Section 5 with some conclusions.

2. Formulation

In this study, natural frequency of a curved FG nano beam as a vibrational characteristic has been investigated based on MCST theory, meanwhile geometrical term $(1 + z / R)$ has been considered. In this way, stress resultants have been obtained and governing equations of motion and related boundary condition have been developed based on Hamilton's principle as in continuance.

2.1 Curved functionally graded nano beams

According to different properties of functionally graded materials (FGMs)in nano-scale such as high stiffness and high thermal resistance in comparison with other materials, these materials are proposed widely in different industries including micro sensors, micro actuators, MEMS and NEMS, aerospace, nuclear power plants and other nuclear projects as a practical material. FGMs mainly are produced by mixing two or more constituents using metallurgy powder method. A certain kind of FGM is a mixture of ceramic and metal in which ceramic constituent is highly thermal resistant due to its low coefficient of thermal conductivity and metal constituent prevents the structure from fracture due to thermal stresses. In laminar composites by applying stresses, some gaps between mismatched layers are created due to different local physical properties, which are called delamination. However structures of FGMs are in such a way that prevents from occurring such phenomenon. Selecting the kind of utilized metal depends on requirements and applications. In the presented report, it has been supposed that volume fraction V in curved FG nanobeam which is made of ceramic and metal varies due to gradient index p in such a way that one thinks the material is graded. This type of grading causes that in radial direction of the beam, distribution of material varies

continuously and gradually in so far as the inner and outer surface of the beam become pure metal and pure

ceramic, respectively. Therefore, it can be said that physical and mechanical properties such as Young's modulus E, Poisson's ratio v and mass density ρ vary through thickness of the curved FG nano beam as following

$$\begin{aligned} E(z) &= E_m - (E_m - E_c)V_c(z) \\ v(z) &= v_m - (v_m - v_c)V_c(z) \\ \rho(z) &= \rho_m - (\rho_m - \rho_c)V_c(z) \end{aligned} \tag{1}$$

Where m and c subscripts denote properties of metallic phase and ceramic phase, respectively. V is volume fraction of material phase. Volume fraction of mixture of metal and ceramic is equal to

$$V_c + V_m = 1 \tag{2}$$

Volume fractions of metal and ceramic constituents have been assumed to be obtained as following

$$V_c(z) = \left(0.5 + \frac{z}{h}\right)^p,\ V_m(z) = 1 - \left(0.5 + \frac{z}{h}\right)^p \tag{3}$$

Where p is a nonnegative quantity (gradient index) that adjusts specifications of materials variation in thickness direction.

2.2 Geometrical properties

In Fig. 1, a curved FG nano beam which is made of ceramic and metal constituents, containing thickness h, radius of curvature R, length L and opening angle α is illustrated.

According to this figure, it is clear that the origin of utilized coordinate system containing x, y and z axis, is located on center of lateral surface (as shown); x axis coincides with curved path of the FG nano beam. In order to derive equations and describing amount of swept opening angle in the beam, this parameter is replaced by relation $x = R\theta$.

According to the figure, y axis is perpendicular to the plane of the paper and directed outward and z axis is along the radius of curvature and directed to its center. Based on first order shear deformation theory, displacement vector, which contains local and time variations of the beam, can be defined as

$$\begin{aligned} \mathrm{u} &= u_\theta \hat{e}_\theta + u_y \hat{e}_y + u_z \hat{e}_z \\ u_\theta &= u(t,\theta) - z\varphi(t,\theta)\ ,\ u_y = 0\ ,\ u_z = w(t,\theta) \end{aligned} \tag{4}$$

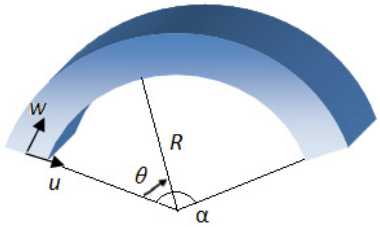

Fig. 1 Schematic of curved nano beam

Where u_θ, u_y and u_z are components of displacement vector u which indicate local variations of mid plane, the plane which is located in R distance from center of curvature and x-y plane, along x, y and z axis, respectively. t is parameter of time and φ describes rotation of mentioned mid plane about y axis.

2.3 Modified couple stress theory

For the first time MCST theory has been concluded by Yang *et al*. (2002) from CCST theory which was proved previously. Considering symmetric rotation gradient tensor and a solo length scale parameter to capture the size effect in nano structures, causes this theory to be preferred in comparison with CCST theory. Consequently, MCST theory has been recently utilized to investigate different nano structures such as Euler- Bernoulli and Timoshenko nano beam, Mindlin's and kirchhoff's nano plates, functionally graded nano beams, etc. Therefore, saved strain energy in region O, due to very small deformations of a continues spectrum in a linear elastic material which consists of strain tensor and curve tensor, can be expressed based on MCST theory as following

$$U_m = \frac{1}{2}\int_{\mathrm{O}} \left(\sigma_{ij}\varepsilon_{ij} + m_{ij}\chi_{ij}\right) dV, \qquad (i,j = \theta, y, z) \tag{5}$$

Where ε_{ij} and χ_{ij} are defined as

$$\varepsilon_{ij} = \frac{1}{2}\left[(\nabla u)_{ij} + (\nabla u)_{ij}^T\right] = \frac{1}{2}\left(u_{i,j} + u_{j,i}\right) = \varepsilon_{ji} \tag{6a}$$

$$\begin{aligned} \chi_{ij} &= \frac{1}{2}\left[(\nabla\theta)_{ij} + (\nabla\theta)_{ij}^T\right] = \frac{1}{2}\left(\theta_{i,j} + \theta_{j,i}\right) = \chi_{ij}, \\ \theta_i &= \frac{1}{2}(\nabla \times u)_i \end{aligned} \tag{6b}$$

In above relations u_i and θ_i are displacement vector u and very small rotation vector θ, respectively. Furthermore, strain tensor ε components and symmetric rotation gradient tensor χ have been introduced by ε_{ij} and χ_{ij}, symbols, respectively. Derived parameters from strain energy density, according to defined kinematical parameters σ and m, have been shown as σ_{ij} and m_{ij}, respectively σ is called classical stress tensor and m is called higher order stress tensor which can be expressed for a homogeneous linear elastic material, using effective kinematical parameters on problem, as following

$$\begin{aligned} \sigma_{ij} &= \lambda tr(\varepsilon_{ij})\delta_{ij} + 2\mu\varepsilon_{ij} \\ m_{ij} &= 2\mu l^2 \chi_{ij} \end{aligned} \tag{7}$$

Where, additional length scale parameter has been shown by l, which is related to symmetric rotation gradient tensor. Also δ is Kroneker's delta. λ and μ are bulk modulus and shear modulus, respectively which can be observed in top relations considering to classical and higher order stress tensors and they are described as following

$$\lambda = \frac{E(z)v(z)}{\left(1+v(z)\right)\left(1-2v(z)\right)}, \qquad \mu = \frac{E(z)}{2\left(1+v(z)\right)} \tag{8}$$

As previously mentioned, E is Young' modulus and v is Poisson's ratio.

2.4 Governing equations of motion and associated boundary conditions

By substituting Eq. (4) into Eqs. (6a)-(6b), nonzero physical components of strain displacement tensor ε and rotational vector θ in curved FG nano beam can be expressed as

$$\begin{gathered}\varepsilon_{\theta\theta} = \frac{\varepsilon_0 - z\varepsilon_1}{\left(1+z/R\right)}, \quad \varepsilon_{\theta z} = \frac{\varepsilon_2}{\left(1+z/R\right)} = \varepsilon_{z\theta}, \\ \varepsilon_{yy} = \varepsilon_{zz} = \varepsilon_{yz} = \varepsilon_{y\theta} = 0 \\ \varepsilon_0 = \frac{1}{R}\frac{\partial u}{\partial\theta} + \frac{w}{R}, \quad \varepsilon_1 = \frac{1}{R}\frac{\partial\varphi}{\partial\theta}, \\ \varepsilon_2 = -\frac{1}{2}\left(\frac{u}{R} - \frac{1}{R}\frac{\partial w}{\partial\theta} + \varphi\right)\end{gathered} \tag{9a}$$

$$\begin{gathered}\theta_y = \frac{1}{2}\left(\varphi + \frac{\theta_0 - z\theta_1}{\left(1+z/R\right)}\right), \qquad \theta_\theta = \theta_z = 0 \\ \theta_0 = \frac{u}{R} - \frac{1}{R}\frac{\partial w}{\partial\theta}, \qquad \theta_1 = \frac{\varphi}{R}\end{gathered} \tag{9b}$$

Consider Eqs. (9a)-(9b). It is observed that geometrical term $(1 + z / R)$ has appeared in strain-displacement relation and the rotational vector. If radius of curvature of the beam R is significantly larger than its thickness h, that is $h / R <<$ 1and therefore $|z / R| << 1$, accordingly $(1 + z / R)$ will be equal to one. However Qatu (2004) represented that if h / R ratio is more than 0.5, influences of geometrical term will be important and should not be neglected and as same as here, this term should be inserted to equations and its influences should be involved in free vibration characteristics of the curved FG nano beam.

Now, by substituting Eq. (9a)-(9b) into Eq. (6b) nonzero components of symmetric rotation gradient tensor χ_{ij} are obtained as following

$$\begin{gathered}\chi_{\theta y} = \frac{1}{4}\left[\frac{\frac{1}{R}\frac{\partial\varphi}{\partial\theta} + \frac{\frac{1}{R^2}\frac{\partial u}{\partial\theta} - \frac{1}{R^2}\frac{\partial^2 w}{\partial\theta^2} - \frac{z}{R^2}\frac{\partial\varphi}{\partial\theta}}{1+z/R}}{}\right] \\ \chi_{yz} = \frac{1}{4}\left[\frac{-\frac{u}{R^2} + \frac{1}{R^2}\frac{\partial w}{\partial\theta} - \frac{\varphi}{R}}{\left(1+z/R\right)^2}\right]\end{gathered} \tag{10}$$

In continuance, classical and higher order stress tensors are obtained by substituting Eqs. (9a) and (10) into Eq. (7). By using following equations, relation considering to stress resultants may be obtained.

$$\begin{gathered}\begin{Bmatrix} N_{\theta\theta} \\ M_{\theta\theta} \\ Q \end{Bmatrix} = \int_{-h/2}^{h/2} \begin{Bmatrix} \sigma_{\theta\theta}\begin{Bmatrix}1\\ z\end{Bmatrix} \\ \sigma_{\theta z}\end{Bmatrix} dz, \\ \begin{Bmatrix} Y_{ij} \\ M_{ij}^m \end{Bmatrix} = \int_{-h/2}^{h/2} m_{ij}^s \begin{Bmatrix}1\\ z\end{Bmatrix} dz,\end{gathered} \tag{11}$$

If obtained classical and higher order stress tensors are substituted into Eq. (11), equations of stress resultants are obtained as below

$$\begin{gathered}N_{\theta\theta} = A_{11}\left(\frac{1}{R}\frac{\partial u}{\partial\theta} + \frac{w}{R}\right) - B_{11}\left(\frac{1}{R}\frac{\partial\varphi}{\partial\theta}\right) \\ Q = k_s A_{55,1}\left(-\frac{u}{R} + \frac{1}{R}\frac{\partial w}{\partial\theta} - \varphi\right) \\ M_{\theta\theta} = B_{11}\left(\frac{1}{R}\frac{\partial u}{\partial\theta} + \frac{w}{R}\right) - D_{11}\left(\frac{1}{R}\frac{\partial\varphi}{\partial\theta}\right)\end{gathered} \tag{12a}$$

$$\begin{gathered}Y_{\theta y} = \frac{l_2^2}{2}\left[\begin{array}{l} A_{55,1}\left(\frac{1}{R^2}\frac{\partial u}{\partial\theta} - \frac{1}{R^2}\frac{\partial^2 w}{\partial\theta^2}\right) \\ -B_{55,1}\left(\frac{1}{R^2}\frac{\partial\varphi}{\partial\theta}\right) + A_{55,2}\left(\frac{1}{R}\frac{\partial\varphi}{\partial\theta}\right)\end{array}\right] \\ M_{\theta y}^m = \frac{l_2^2}{2}\left[\begin{array}{l} B_{55,1}\left(\frac{1}{R^2}\frac{\partial u}{\partial\theta} - \frac{1}{R^2}\frac{\partial^2 w}{\partial\theta^2}\right) \\ -D_{55,1}\left(\frac{1}{R^2}\frac{\partial\varphi}{\partial\theta}\right) + B_{55,2}\left(\frac{1}{R}\frac{\partial\varphi}{\partial\theta}\right)\end{array}\right] \\ Y_{yz} = -\frac{l_2^2}{2}\left[A_{55,2}\left(\frac{u}{R^2} - \frac{1}{R^2}\frac{\partial w}{\partial\theta} + \frac{\varphi}{R}\right)\right]\end{gathered} \tag{12b}$$

Stiffness coefficients, which have appeared in above equations, become as follows

$$\begin{gathered}\begin{Bmatrix} A_{11} \\ B_{11} \\ D_{11} \end{Bmatrix} = \int_{-h/2}^{h/2} \left(\lambda + 2\mu\right)\left(1+\frac{z}{R}\right)^{-1} \begin{Bmatrix}1\\ z\\ z^2\end{Bmatrix} dz \\ \begin{Bmatrix} A_{55,1} \\ B_{55,1} \\ D_{55,1} \end{Bmatrix} = \int_{-h/2}^{h/2} \mu\left(1+\frac{z}{R}\right)^{-1} \begin{Bmatrix}1\\ z\\ z^2\end{Bmatrix} dz \\ \begin{Bmatrix} A_{55,2} \\ B_{55,2} \\ D_{55,2} \end{Bmatrix} = \int_{-h/2}^{h/2} \mu\left(1+\frac{z}{R}\right)^{-2} \begin{Bmatrix}1\\ z\\ z^2\end{Bmatrix} dz\end{gathered} \tag{13}$$

Hamilton's principle, which is a generalized case of virtual work theorem, is defined as

$$\int_{t_1}^{t_2} \left[\delta K_T + \delta W_P - \delta U_m\right] dt = 0 \tag{14}$$

Where K_T, W_P and U_m are kinetic energy, potential

energy and strain energy, respectively. By utilizing displacement vector (Eq. (4)), kinetic energy T is described as following in which ρ is mass density and it is obtained from Eq. (1) and A is cross- sectional area of the curved FG nano beam.

$$\begin{aligned} K_T &= \frac{1}{2}\int_A \int_{-h/2}^{h/2} \rho(z)\left\{ {u_{\theta,t}}^2 + {u_{y,t}}^2 + {u_{z,t}}^2 \right\} dzdA \\ &= \frac{1}{2}\int_A \left\{ \begin{array}{l} L_1\left(\left(\frac{\partial u}{\partial t}\right)^2 + \left(\frac{\partial w}{\partial t}\right)^2 \right) \\ -2L_2\left(\frac{\partial u}{\partial t}\frac{\partial \varphi}{\partial t}\right) + L_3\left(\frac{\partial \varphi}{\partial t}\right)^2 \end{array} \right\} dA \end{aligned} \tag{15}$$

L_1, L_2 and L_3 parameters have been defined, respectively as following

$$\begin{aligned} L_i &= \int_{-h/2}^{h/2} \rho(z) z^{i-1} dz, \quad i = 1,2,3 \\ L_1 &= \left(\rho_m h + \frac{(\rho_c - \rho_m)h}{p+1} \right), \\ L_2 &= \frac{1}{2}\left(\frac{p(\rho_c - \rho_m)h^2}{(p+1)(p+2)} \right) \\ L_3 &= \left(\frac{\left((p+1)^2 - (p-1)\right)(\rho_c - \rho_m)h^3}{4(p+1)(p+2)(p+3)} + \rho_m \frac{h^3}{12} \right) \end{aligned} \tag{16}$$

Also, potential energy W_p which is created due to radial load q, can be expressed as

$$W_P = \frac{1}{2}\int_A qw dA \tag{17}$$

As previously mentioned, inserting Eqs. (9a) and (10) into Eq. (7) yields classical and higher order stress tensors. By substituting these tensors and Eq. (6) into Eq. (5), total strain energy is concluded as following

$$\begin{aligned} U_m &= \frac{1}{2}\int_A \int_{-h/2}^{h/2} \left(\sigma_{ij}\varepsilon_{ij} + m_{ij}\chi_{ij} \right) dzdA \\ &= \frac{1}{2}\int_A \int_{-h/2}^{h/2} \left(\begin{array}{l} \sigma_{\theta\theta}\varepsilon_{\theta\theta} + 2\sigma_{\theta z}\varepsilon_{\theta z} \\ +2m_{\theta y}\chi_{\theta y} + 2m_{yz}\chi_{yz} \end{array} \right) dzdA \\ &= \frac{1}{2}\int_A \left\{ \begin{array}{l} N_{\theta\theta}\left(\frac{1}{R}\frac{\partial u}{\partial \theta} + \frac{w}{R}\right) - M_{\theta\theta}\left(\frac{1}{R}\frac{\partial \varphi}{\partial \theta}\right) \\ -Q\left(\frac{u}{R} - \frac{1}{R}\frac{\partial w}{\partial \theta} + \varphi\right) - \frac{M_{\theta y}^m}{2}\left(\frac{1}{R^2}\frac{\partial \varphi}{\partial \theta}\right) \\ +\frac{Y_{\theta y}}{2}\left(\frac{1}{R^2}\frac{\partial u}{\partial \theta} - \frac{1}{R^2}\frac{\partial^2 w}{\partial \theta^2} + \frac{1}{R}\frac{\partial \varphi}{\partial \theta}\right) \\ -\frac{Y_{yz}}{2}\left(\frac{u}{R^2} - \frac{1}{R^2}\frac{\partial w}{\partial \theta} + \frac{\varphi}{R}\right) \end{array} \right\} dA \end{aligned} \tag{18}$$

Where U_m is energy due to strain of all stress tensors. After employing Hamilton's principle, governing equations of motion is obtained as

$$\frac{1}{R}\frac{\partial N_{\theta\theta}}{\partial \theta} + \frac{Q}{R} + \frac{1}{2R^2}\frac{\partial Y_{\theta y}}{\partial \theta} + \frac{Y_{yz}}{2R^2} = L_1\frac{\partial^2 u}{\partial t^2} - L_2\frac{\partial^2 \varphi}{\partial t^2} \tag{19a}$$

$$\frac{1}{R}\frac{\partial Q}{\partial \theta} - \frac{N_{\theta\theta}}{R} + \frac{1}{2R^2}\frac{\partial^2 Y_{\theta y}}{\partial \theta^2} + \frac{1}{2R^2}\frac{\partial Y_{yz}}{\partial \theta} + q = L_1\frac{\partial^2 w}{\partial t^2} \tag{19b}$$

$$\begin{aligned} &-\frac{1}{R}\frac{\partial M_{\theta\theta}}{\partial \theta} + Q + \frac{1}{2R}\frac{\partial Y_{\theta y}}{\partial \theta} - \frac{1}{2R^2}\frac{\partial M_{\theta y}^m}{\partial \theta} + \frac{Y_{yz}}{2R} \\ &= L_3\frac{\partial^2 \varphi}{\partial t^2} - L_2\frac{\partial^2 u}{\partial t^2} \end{aligned} \tag{19c}$$

Moreover, related boundary conditions are derived as following

$$\delta u = 0 \quad or \quad \left\{ -\frac{N_{\theta\theta}}{R} - \frac{Y_{\theta y}}{2R^2} \right\} = 0 \tag{20a}$$

$$\delta w = 0 \quad or \quad \left\{ -\frac{Q}{R} - \frac{1}{2R^2}\frac{\partial Y_{\theta y}}{\partial \theta} - \frac{Y_{yz}}{2R^2} \right\} = 0 \tag{20b}$$

$$\delta \varphi = 0 \quad or \quad \left\{ \frac{M_{\theta\theta}}{R} - \frac{Y_{\theta y}}{2R} + \frac{M_{\theta y}^m}{2R^2} \right\} = 0 \tag{20c}$$

In order to reach final form of governing equations of motion, Eq. (12) is inserted into Eq. (19) and finally following equations are obtained

$$\begin{aligned} &A_{11}\left(\frac{1}{R^2}\frac{\partial^2 u}{\partial \theta^2} + \frac{1}{R^2}\frac{\partial w}{\partial \theta}\right) - B_{11}\left(\frac{1}{R^2}\frac{\partial^2 \varphi}{\partial \theta^2}\right) \\ &-\left(k_s A_{55,1} + SA_{55,2}\right)\left(\frac{u}{R^2} - \frac{1}{R^2}\frac{\partial w}{\partial \theta} + \frac{\varphi}{R}\right) \\ &+\left(\frac{SA_{55,1}}{R^2}\right)\frac{\partial^2 u}{\partial \theta^2} + \left(\frac{SA_{55,2}}{R} - \frac{SB_{55,1}}{R^2}\right)\frac{\partial^2 \varphi}{\partial \theta^2} \\ &-\left(\frac{SA_{55,1}}{R^2}\right)\frac{\partial^3 w}{\partial \theta^3} = L_1\frac{\partial^2 u}{\partial t^2} - L_2\frac{\partial^2 \varphi}{\partial t^2} \end{aligned} \tag{21a}$$

$$\begin{aligned} &-A_{11}\left(\frac{1}{R^2}\frac{\partial u}{\partial \theta} + \frac{w}{R^2}\right) + B_{11}\left(\frac{1}{R^2}\frac{\partial \varphi}{\partial \theta}\right) \\ &-\left(k_s A_{55,1} + SA_{55,2}\right)\left(\frac{1}{R^2}\frac{\partial u}{\partial \theta} - \frac{1}{R^2}\frac{\partial^2 w}{\partial \theta^2} + \frac{1}{R}\frac{\partial \varphi}{\partial \theta}\right) \\ &+\left(\frac{SA_{55,1}}{R^2}\right)\frac{\partial^3 u}{\partial \theta^3} + \left(\frac{SA_{55,2}}{R} - \frac{SB_{55,1}}{R^2}\right)\frac{\partial^3 \varphi}{\partial \theta^3} \\ &-\frac{SA_{55,1}}{R^2}\frac{\partial^4 w}{\partial \theta^4} + q = L_1\frac{\partial^2 w}{\partial t^2} \end{aligned} \tag{21b}$$

$$+\left(\frac{SA_{55,1}}{R} - \frac{SB_{55,1}}{R^2}\right)\frac{\partial^2 u}{\partial \theta^2} - \left(\frac{SA_{55,1}}{R} - \frac{SB_{55,1}}{R^2}\right)\frac{\partial^3 w}{\partial \theta^3} \tag{21c}$$

$$
\begin{aligned}
&-B_{11}\left(\frac{1}{R^2}\frac{\partial^2 u}{\partial\theta^2}+\frac{1}{R^2}\frac{\partial w}{\partial\theta}\right)+D_{11}\left(\frac{1}{R^2}\frac{\partial^2\varphi}{\partial\theta^2}\right)\\
&+\left(SA_{55,2}-\frac{SB_{55,1}+SB_{55,2}}{R}+\frac{SD_{55,1}}{R^2}\right)\frac{\partial^2\varphi}{\partial\theta^2}\\
&-\left(k_s A_{55,1}+SA_{55,2}\right)\left(\frac{u}{R}-\frac{1}{R}\frac{\partial w}{\partial\theta}+\varphi\right)\\
&=L_3\frac{\partial^2\varphi}{\partial t^2}-L_2\frac{\partial^2 u}{\partial t^2}
\end{aligned}
\tag{21c}
$$

Also, in order to obtain final form of related boundary conditions, Eq. (12) is substituted into Eq. (20) as

$$
\begin{aligned}
&-A_{11}\left(\frac{1}{R^2}\frac{\partial u}{\partial\theta}+\frac{w}{R^2}\right)+B_{11}\left(\frac{1}{R^2}\frac{\partial\varphi}{\partial\theta}\right)-\left(\frac{SA_{55,1}}{R^2}\right)\frac{\partial u}{\partial\theta}\\
&-\left(\frac{SA_{55,2}}{R}-\frac{SB_{55,1}}{R^2}\right)\frac{\partial\varphi}{\partial\theta}+\left(\frac{SA_{55,1}}{R^2}\right)\frac{\partial^2 w}{\partial\theta^2}=0
\end{aligned}
\tag{22a}
$$

$$
\begin{aligned}
&\left(k_s A_{55,1}+SA_{55,2}\right)\left(\frac{u}{R^2}-\frac{1}{R^2}\frac{\partial w}{\partial\theta}+\frac{\varphi}{R}\right)+\frac{SA_{55,1}}{R^2}\frac{\partial^3 w}{\partial\theta^3}\\
&-\left(\frac{SA_{55,1}}{R^2}\right)\frac{\partial^2 u}{\partial\theta^2}-\left(\frac{SA_{55,2}}{R}-\frac{SB_{55,1}}{R^2}\right)\frac{\partial^2\varphi}{\partial\theta^2}=0
\end{aligned}
\tag{22b}
$$

$$
\begin{aligned}
&B_{11}\left(\frac{1}{R^2}\frac{\partial u}{\partial\theta}+\frac{w}{R^2}\right)-D_{11}\left(\frac{1}{R^2}\frac{\partial\varphi}{\partial\theta}\right)\\
&-\left(\frac{SA_{55,2}-SB_{55,2}}{R}-\frac{SB_{55,1}-SD_{55,1}}{R^2}\right)\frac{\partial\varphi}{\partial\theta}\\
&-\left(\frac{SA_{55,1}-SB_{55,1}}{R^2}\right)\frac{\partial u}{\partial\theta}+\left(\frac{SA_{55,1}-SB_{55,1}}{R^2}\right)\frac{\partial^2 w}{\partial\theta^2}=0
\end{aligned}
\tag{22c}
$$

Where, utilized coefficients are expressed as following

$$
S=\frac{l^2}{4R^2} \tag{23}
$$

3. Closed-form solution

As a case study, by employing Navier's solution method, free vibration problem of a curved FG nano beam, by assuming $q = 0$, has been investigated. Simply supported boundary condition on $\theta = 0$, α edges can be expressed as follows

$$
\begin{aligned}
&N_{\theta\theta}+\frac{Y_{\theta y}}{2R}=\frac{1}{R}\frac{\partial u}{\partial\theta}=w=\frac{Y_{\theta y}}{2}=0\\
&M_{\theta\theta}+\frac{Y_{\theta y}}{2}=\frac{1}{R}\frac{\partial\varphi}{\partial\theta}=0
\end{aligned}
\tag{24}
$$

Based on Navier's solution method, components containing acceptable displacement, which satisfy aforesaid governing equations and simply supported boundary condition, identically, are considered as

$$
u(t,\theta)=\sum_{n=1}^{\infty}U_n\cos\left(\frac{n\pi\theta}{\alpha}\right)e^{i\omega t} \tag{25}
$$

$$
\begin{aligned}
w(t,\theta)&=\sum_{n=1}^{\infty}W_n\sin\left(\frac{n\pi\theta}{\alpha}\right)e^{i\omega t}\\
\varphi(t,\theta)&=\sum_{n=1}^{\infty}\Psi_n\cos\left(\frac{n\pi\theta}{\alpha}\right)e^{i\omega t}
\end{aligned}
\tag{25}
$$

Where ω_n is natural frequency of the curved FG nano beam and integer number n denotes nth mode number. By substituting Eq. (25) into Eq. (21) and using trigonometric relations, three algebraic equations will be obtained

$$
\begin{aligned}
&\left\{\left[K_{ij}\right]-\omega^2\left[L\right]\right\}\left\{M_n\right\}=0,\quad (i,j=1,2,3)\\
&\left[K_{ij}\right]=\begin{bmatrix}K_{11}&K_{12}&K_{13}\\K_{21}&K_{22}&K_{23}\\K_{31}&K_{32}&K_{33}\end{bmatrix}\\
&\left[L\right]=\begin{bmatrix}L_1&0&-L_2\\0&L_1&0\\-L_2&0&L_3\end{bmatrix},\quad \left\{M_n\right\}=\begin{Bmatrix}U_n\\W_n\\\Psi_n\end{Bmatrix}
\end{aligned}
\tag{26}
$$

Where amounts of K_{ij} are calculated as following

$$
\begin{aligned}
K_{11}&=-\frac{k_s A_{55,1}}{R^2}-\frac{SA_{55,2}}{R^2}-\left(\frac{A_{11}+SA_{55,1}}{R^2}\right)\Theta^2\\
K_{12}&=K_{21}=\left(\frac{A_{11}+k_s A_{55,1}+SA_{55,2}}{R^2}\right)\Theta+\left(\frac{SA_{55,1}}{R^2}\right)\Theta^3\\
K_{13}&=K_{31}=-\frac{k_s A_{55,1}}{R}-\left(\frac{SA_{55,2}}{R}-\frac{B_{11}+SB_{55,1}}{R^2}\right)\Theta^2\\
&\quad-\frac{SA_{55,2}}{R}\\
K_{22}&=-\frac{A_{11}}{R^2}-\left(\frac{k_s A_{55,1}+SA_{55,2}}{R^2}\right)\Theta^2-\frac{SA_{55,1}}{R^2}\Theta^4\\
K_{23}&=K_{32}=\left(\frac{k_s A_{55,1}+SA_{55,2}}{R}-\frac{B_{11}}{R^2}\right)\Theta\\
&\quad+\left(\frac{SA_{55,2}}{R}-\frac{SB_{55,1}}{R^2}\right)\Theta^3\\
K_{33}&=-\left(SA_{55,2}-\frac{SB_{55,1}+SB_{55,2}}{R}+\frac{D_{11}+SD_{55,1}}{R^2}\right)\Theta^2\\
&\quad-k_s A_{55,1}-SA_{55,2}
\end{aligned}
\tag{27}
$$

Where, utilized coefficients are expressed as following

$$
\Theta=\frac{n\pi}{\alpha} \tag{28}
$$

By solving obtained eigenvalue problem in Eq. (26), numerically, natural frequency of the curved FG nano beam can be determined.

4. Results and discussion

Accomplished study has been performed based on MCST theory, in order to show influences of involved

Table 1 Validation of the presented results about natural frequency of the curved FG nano-beam with reference and differences between them for various values of mode number and h / l ($k_s = 5/6$, $R = L / \alpha$, $\alpha = \pi / 4$, $p = 1.2$, $L = 20\ h$, $l = 15\ \mu$m)

n		h / l						
		1	2	3	4	6	8	10
1	Present	1.47078	0.452186	0.250943	0.172971	0.107467	0.0784347	0.0619295
	Ref (Ansari *et al*. 2013)	1.4716	0.4524	0.251	0.1729	0.1074	0.0784	0.0619
	Difference	-0.0558	-0.0473	-0.0227	0.041	0.0623	0.0446	0.0484
2	Present	6.19012	1.91633	1.06452	0.733925	0.45603	0.332839	0.2628
	Ref (Ansari *et al*. 2013)	6.1914	1.9167	1.0644	0.7337	0.4558	0.3326	0.2626
	Difference	-0.0207	-0.0193	0.0113	0.0307	0.0504	0.0718	0.0761
3	Present	13.6851	4.27859	2.37995	1.64132	1.01995	0.744422	0.587769
	Ref (Ansari *et al*. 2013)	13.6835	4.2784	2.3793	1.6406	1.0193	0.7439	0.5874
	Difference	0.0117	0.0044	0.0273	0.0439	0.0637	0.0701	0.0628

parameters on one of the most important vibration characteristics of a curved FG nano beam, that is natural frequency. Properties of the curved FG nano beam vary in radial direction due to value of gradient index p, in such a way that inner and outer surface of the beam is rich from ceramic and rich from metal, respectively. In this work, structural materials of the curved FG nano beam have been assumed to be Aluminum with $E_m = 70$ GPa, $\nu_m = 0.3$ and $\rho_m = 2702$ kg/m^3 and SiC with $E_c = 427$ GPa, $\nu_c = 0.17$, $\rho_c = 3100$ kg/m^3.

It should be pointed out that magnitude of length scale parameter for a homogenous isotropic nano beam was obtained experimentally in laboratory as $L = 17.6\ \mu$m by Lam *et al*. (2003).

However there is no reliable numerical result for length scale parameter of a curved FG nano beam. According to this fact, in order to analyze the problem, numerically, approximate magnitude of related length scale parameter has been assumed to be $L = 15\ \mu$m in this case. Similar assumption can be found in Ref. (Şimşek and Reddy 2013). If the thickness of a curved FG nano beam h is far smaller than its radius of curvature R, that is $h / R << 1$, geometrical term $(1 + z / R)$ can be assumed to be equal to one with an excellent approximation. However, by noting to the work done by Qatu *et al*. (Qatu 2004, Hajianmaleki and Qatu 2012) in this field, it can be said that, if h / R ratio is larger than 0.5, influences of deepness term should not be neglected and the term should be involved in calculations.

To the authors' knowledge, there is no profound study and report about free vibration of a curved FG nano beam based on MCST theory, together with inclusion of geometrical term $(1 + z / R)$, in previously published papers. Accordingly, such results have been presented with which other researchers can compare their results on future.

Validation of obtained results has been investigated bycomparing the results with those of previous works.Errors percentage and difference percentage between presented results and those of previous works due to neglecting geometrical term $(1 + z / R)$ have been reported in tabulated and graphical data. These differences percentage are described as $diff = [(\omega_{presented} - \omega_{ref}) / \omega_{presented}] \times 100\%$. In this work a profound and adequate study has been performed on influences of involved parameters in the problem such as dimensionless length scale parameter h / l, aspect ratio L / h, opening angle α, mode number n, gradient index p and variations of these parameters and also interactive influences of them on natural frequency of the curved FG nano beam ω_n. In continuance, conclusions from analysis of tabulated data will be discussed.

In Table 1 presented results have been compared with those by Ansari *et al*. (2013). This table represents influences of increasing the dimensionless ratio h/l on natural frequency for various mode numbers. According to Ref. (Ansari *et al*. 2013), values of effective parameter have been assumed to be $k_s = 5/6$, $R = L / \alpha$, $\alpha = \pi / 4$, $p = 1.2$, $L = 20\ h$, $l = 15\ \mu$m. It is observed that an increase in h/l leads to a reduction of natural frequency ω_n. This effect continues approximately in an exponential pattern, with a negative rate. Increasing of mode number causes the dependency of ω_n on h / l to increase and its rate increases exponentially.

Differences of presented results and those of Ref.

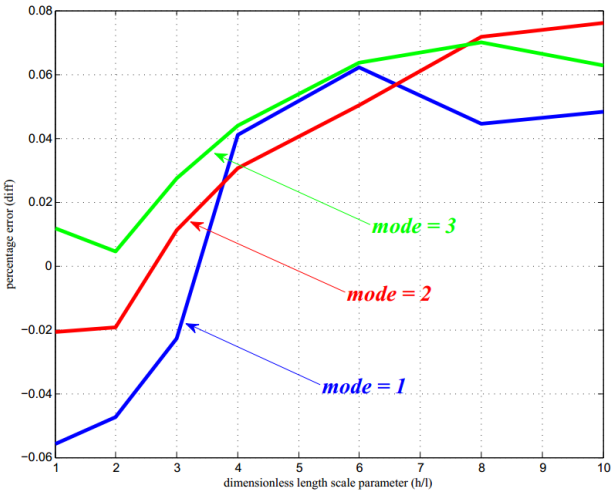

Fig. 2 Differences between results by Ref. (Ansari *et al*. 2013) and presented results for various values of mode number and h/l for the case in which $k_s = 5/6$, $R = L / \alpha$, $\alpha = \pi / 4$, $p = 1.2$, $L = 20\ h$, $l = 15\ \mu$m

(Ansari *et al*. 2013) can be observed in Fig. 2 and Table 1. Generally, for first and second modes, presented natural frequencies are initially smaller than those of Ref. (Ansari *et al*. 2013) and in continuance by increasing h / l, results coincide on a point with together and then finally, presented results become larger than those of Ansari *et al*. (2013). However for third mode it is observed that, reported natural frequencies for none of values of h / l coincide with those of (Ansari *et al*. 2013) and always are larger. It can be said that the most differences percentage for first, second and third modes are 0.0623% for $h / l = 6$, 0.0761% for $h / l = 10$ and 0.0701% for $h / l = 8$, respectively. However the least difference percentage is 0.0044% for $h / l = 2$ which relates to third mode number.

Coincidence of two groups of data occurs in a point between $h / l = 3$ and $h / l = 4$ for the first mode and between $h / l = 2$ and $h / l = 3$ for the second mode. According to Table 1, the most and the least differences percentage are 0.0761% for $n = 2$ and $h / l = 10$ and 0.0044% for $n = 3$ and $h / l = 2$, respectively.

Coincidence and differences of presented results and those of Ref. (Ansari *et al*. 2013) have been illustrated in

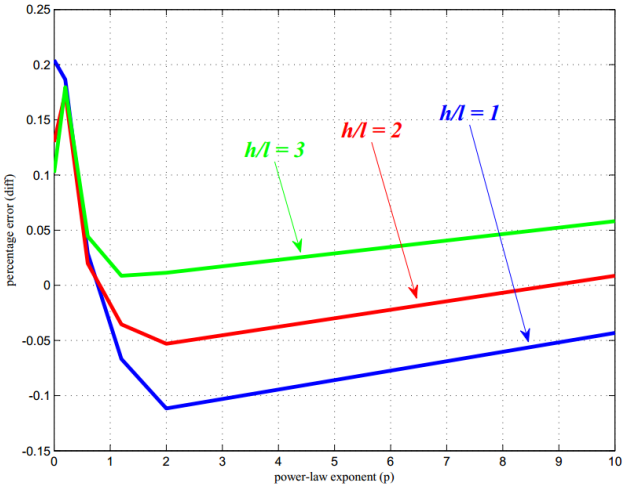

Fig. 4 Differences between Ref. (Ansari *et al*. 2013) and presented results for various values of h/l and p for the case in which $k_s = 5 / 6$, $R = L / \alpha$, $\alpha = \pi / 4$, $n = 1$, $L = 15\ h$, $b = 2\ h$, $l = 15\ \mu$m

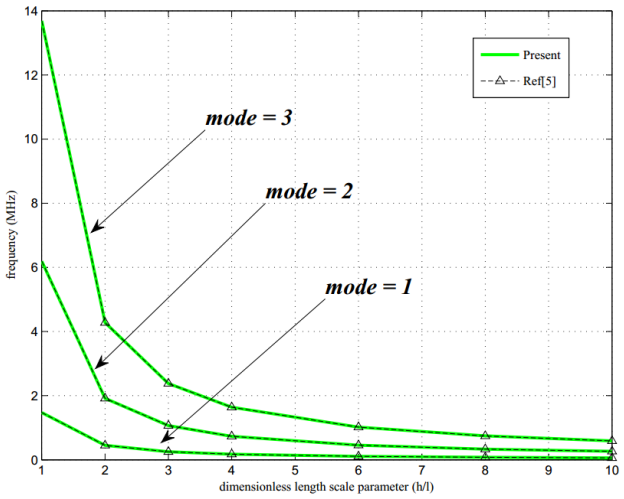

Fig. 3 Coincidence of results by Ref. (Ansari *et al*. 2013) with presented results

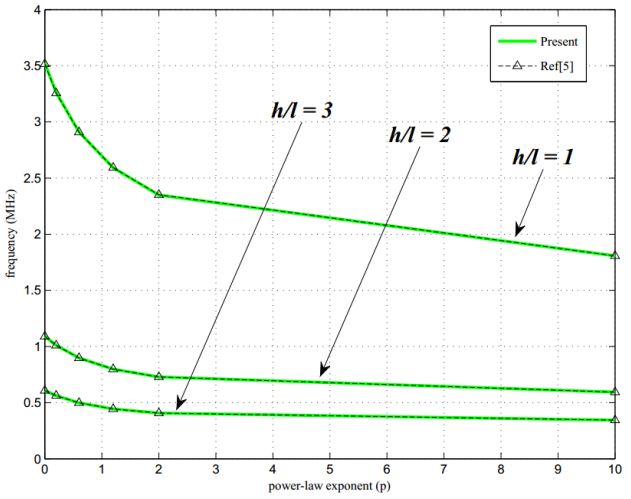

Fig. 5 Coincidence of results by Ref. (Ansari *et al*. 2013) with presented results

Table 2 Validation of the presented results about natural frequency of the curve FG nano-beam with reference and differences between them for various values of p and h / l ($k_s = 5 / 6$, $R = L / \alpha$, $\alpha = \pi / 4$, $n = 1$, $L = 15\ h$, $b = 2\ h$, $l = 15\ \mu$m)

h / l		P						
		1	2	3	4	6	8	10
1	Present	3.52229	3.26299	2.90954	2.59077	2.34828	1.80662	3.52229
	Ref (Ansari *et al*. 2013)	3.5151	3.2569	2.9087	2.5925	2.3509	1.8074	3.5151
	Difference	0.2041	0.1866	0.0289	-0.0668	-0.1116	-0.0432	0.2041
2	Present	1.09192	1.01066	0.897878	0.798617	0.728714	0.594251	1.09192
	Ref (Ansari *et al*. 2013)	1.0905	1.0089	0.8977	0.7989	0.7291	0.5942	1.0905
	Difference	0.13	0.1741	0.0198	-0.0354	-0.053	0.0086	0.13
3	Present	0.608621	0.563011	0.498921	0.443438	0.406546	0.344	0.608621
	Ref (Ansari *et al*. 2013)	0.608	0.562	0.4987	0.4434	0.4065	0.3438	0.608
	Difference	0.102	0.1796	0.0443	0.0086	0.0113	0.0581	0.102

Table 3 Natural frequencies ω_n of the curved FG nano-beam for $b = 2\,h$ and various values of n, h / l, L / h, α for the case in which $p = 0$

h/l	ω_n	$L/h = 10$				$L/h = 20$			
		$\alpha = \pi/6$	$\alpha = \pi/4$	$\alpha = \pi/3$	$\alpha = \pi/2$	$\alpha = \pi/6$	$\alpha = \pi/4$	$\alpha = \pi/3$	$\alpha = \pi/2$
1	$n = 1$	8.23157	7.79359	7.21246	5.71935	2.10267	1.99331	1.84726	1.46827
	$n = 2$	31.6901	31.2142	30.5642	28.7994	8.50457	8.38984	8.23157	7.79359
	$n = 3$	65.5968	65.0717	64.3524	62.3892	18.6589	18.5412	18.3778	17.9195
2	$n = 1$	2.56502	2.43259	2.25559	1.7955	0.649925	0.616385	0.571509	0.454712
	$n = 2$	10.0908	9.9583	9.77543	9.26869	2.6471	2.61265	2.56502	2.43259
	$n = 3$	21.3813	21.2534	21.0758	20.577	5.86616	5.83204	5.78457	5.65069
4	$n = 1$	0.988804	0.938141	0.870309	0.693466	0.250172	0.237286	0.220038	0.175113
	$n = 2$	3.90324	3.8538	3.7854	3.59497	1.02016	1.007	0.988804	0.938141
	$n = 3$	8.2911	8.24539	8.18174	8.00208	2.2645	2.2516	2.23365	2.18295
8	$n = 1$	0.449917	0.426908	0.396088	0.315681	0.11381	0.107951	0.100107	0.079673
	$n = 2$	1.77621	1.75391	1.72304	1.63701	0.464153	0.45818	0.449917	0.426908
	$n = 3$	3.77054	3.75017	3.7218	3.64162	1.03041	1.02457	1.01644	0.993481
16	$n = 1$	0.219034	0.207838	0.192839	0.153701	0.055406	0.052553	0.048735	0.038788
	$n = 2$	0.864649	0.853818	0.838823	0.797022	0.22596	0.223055	0.219034	0.207838
	$n = 3$	1.83487	1.82501	1.81127	1.77243	0.501619	0.498781	0.494828	0.483664

Table 4 Natural frequencies ω_n of the curved FG nano-beam for $b = 2\,h$ and various values of n, h / l, L / h, α for the case in which $p = 0.1$

h/l	ω_n	$L/h = 10$				$L/h = 20$			
		$\alpha = \pi/6$	$\alpha = \pi/4$	$\alpha = \pi/3$	$\alpha = \pi/2$	$\alpha = \pi/6$	$\alpha = \pi/4$	$\alpha = \pi/3$	$\alpha = \pi/2$
1	$n = 1$	7.90585	7.47887	6.91595	5.47728	2.02128	1.91529	1.77421	1.40922
	$n = 2$	30.4421	29.9607	29.3147	27.5852	8.17562	8.06152	7.90585	7.47887
	$n = 3$	63.0304	62.4821	61.7516	59.8	17.9383	17.8169	17.652	17.1973
2	$n = 1$	2.463	2.33389	2.16243	1.71915	0.624618	0.592131	0.548806	0.436363
	$n = 2$	9.6908	9.55551	9.3724	8.87299	2.54408	2.50984	2.463	2.33389
	$n = 3$	20.5378	20.3987	20.2126	19.7051	5.63815	5.60286	5.5548	5.42161
4	$n = 1$	0.949306	0.899984	0.834335	0.664046	0.240369	0.227901	0.211261	0.168031
	$n = 2$	3.74782	3.69746	3.62908	3.44157	0.980206	0.967167	0.949306	0.899984
	$n = 3$	7.9625	7.91275	7.84595	7.66279	2.17592	2.16265	2.14453	2.09421
8	$n = 1$	0.431907	0.409526	0.379715	0.302311	0.109337	0.10367	0.096106	0.076448
	$n = 2$	1.70533	1.68267	1.65187	1.56726	0.445916	0.440007	0.431907	0.409526
	$n = 3$	3.62078	3.59869	3.56899	3.48739	0.989974	0.983984	0.975803	0.953049
16	$n = 1$	0.210261	0.199373	0.184867	0.147195	0.053225	0.050468	0.046786	0.037217
	$n = 2$	0.830122	0.819127	0.804173	0.763075	0.217074	0.2142	0.210261	0.199373
	$n = 3$	1.76194	1.75126	1.7369	1.6974	0.481915	0.479006	0.475031	0.463973

Fig. 3. It is observed that for larger values of h/l, natural frequency approaches to a constant and negligible amount.

In Table 2 presented results which are related to influences of p variations on natural frequency of the curved FG nano beam for various values of h/l ratio, have been compared with those of Ref. (Ansari *et al*. 2013). Effective parameters on problem as Ref. (Ansari *et al*. 2013) are assumed to be $k_s = 5 / 6$, $R = L / \alpha$, $\alpha = \pi / 4$, $n = 1$, $L = 15\,h$, $b = 2\,h$, $l = 15\,\mu$m. In an overview it can be said that increasing of p leads to an increase in ω_n. However, by increasing of h / l, rate of this procedure descends.

Consider Fig. 4. It is clear that due to ignoring geometrical term $(1 + z / R)$ by Ansari *et al*. (2013), presented data are initially larger than those of Ref. (Ansari *et al*. 2013) for $h / l = 1$ and $h / l = 2$, then they coincide at a point between $p = 0.6$ and $p = 1.2$ for $h / l = 1$ and $h / l = 2$ and in continuance they become smaller than those of Ref. (Ansari *et al*. 2013). At last by crossing from $p = 2$ to $p = 10$ differences between results diminishes again. However it is observed that although the results which are related to $h / l = 3$ have an identical pattern but they are always more than those of Ref. (Ansari *et al*. 2013) and for none of p values,

Table 5 Natural frequencies ω_n of the curved FG nano-beam for $b = 2h$ and various values of n, h/l, L/h, α for the case in which $p = 0.2$

h/l	ω_n	$L/h = 10$				$L/h = 20$			
		$\alpha = \pi/6$	$\alpha = \pi/4$	$\alpha = \pi/3$	$\alpha = \pi/2$	$\alpha = \pi/6$	$\alpha = \pi/4$	$\alpha = \pi/3$	$\alpha = \pi/2$
1	$n = 1$	7.62578	7.2085	6.66146	5.26983	1.9512	1.84814	1.71138	1.35847
	$n = 2$	29.3701	28.8849	28.2432	26.5453	7.89247	7.77906	7.62578	7.2085
	$n = 3$	60.8295	60.2629	59.524	57.584	17.3182	17.1941	17.0282	16.5771
2	$n = 1$	2.37412	2.24801	2.08147	1.65293	0.602536	0.57098	0.52902	0.420387
	$n = 2$	9.34275	9.20544	9.02253	8.53027	2.45422	2.42021	2.37412	2.24801
	$n = 3$	19.8051	19.6572	19.4645	18.951	5.43936	5.40317	5.35474	5.22238
4	$n = 1$	0.914396	0.866302	0.80262	0.638163	0.23169	0.219596	0.203499	0.161775
	$n = 2$	3.61063	3.55964	3.49146	3.30686	0.944845	0.931933	0.914396	0.866302
	$n = 3$	7.67297	7.62002	7.55082	7.36533	2.09757	2.08401	2.06581	2.01592
8	$n = 1$	0.415874	0.394071	0.365175	0.290464	0.105347	0.099855	0.092541	0.073578
	$n = 2$	1.64231	1.61942	1.58875	1.50555	0.429658	0.423816	0.415874	0.394071
	$n = 3$	3.48786	3.46442	3.43371	3.35119	0.953946	0.947845	0.939643	0.917122
16	$n = 1$	0.202432	0.191829	0.177772	0.141417	0.051277	0.048604	0.045045	0.035816
	$n = 2$	0.799351	0.788252	0.773374	0.732979	0.209133	0.206293	0.202432	0.191829
	$n = 3$	1.69706	1.68574	1.6709	1.63099	0.464317	0.461357	0.457375	0.446436

Table 6 Natural frequencies ω_n of the curved FG nano-beam for $b = 2h$ and various values of n, h/l, L/h, α for the case in which $p = 0.5$

h/l	ω_n	$L/h = 10$				$L/h = 20$			
		$\alpha = \pi/6$	$\alpha = \pi/4$	$\alpha = \pi/3$	$\alpha = \pi/2$	$\alpha = \pi/6$	$\alpha = \pi/4$	$\alpha = \pi/3$	$\alpha = \pi/2$
1	$n = 1$	6.97247	6.57908	6.07004	4.78927	1.7874	1.69135	1.56482	1.24031
	$n = 2$	26.8698	26.3802	25.7526	24.1352	7.23059	7.11952	6.97247	6.57908
	$n = 3$	55.7001	55.0987	54.3472	52.4451	15.8689	15.7398	15.5732	15.1333
2	$n = 1$	2.16449	2.0459	1.89131	1.49796	0.550335	0.521036	0.482346	0.382771
	$n = 2$	8.52189	8.38162	8.20095	7.72874	2.24179	2.20859	2.16449	2.0459
	$n = 3$	18.0778	17.9127	17.7082	17.1875	4.96946	4.93167	4.88287	4.75353
4	$n = 1$	0.83106	0.786074	0.72723	0.576854	0.210924	0.199748	0.184967	0.146865
	$n = 2$	3.28314	3.23139	3.1644	2.98808	0.860241	0.847731	0.83106	0.786074
	$n = 3$	6.98205	6.92296	6.84952	6.66145	1.91011	1.89609	1.8779	1.82947
8	$n = 1$	0.377368	0.357035	0.3304	0.262226	0.095743	0.09068	0.08398	0.066696
	$n = 2$	1.49096	1.46785	1.43785	1.35865	0.390527	0.384891	0.377368	0.357035
	$n = 3$	3.16871	3.14271	3.11028	3.02693	0.867231	0.860961	0.852805	0.831035
16	$n = 1$	0.183595	0.173716	0.16077	0.127618	0.046577	0.044115	0.040857	0.032451
	$n = 2$	0.725316	0.714129	0.699594	0.661187	0.189983	0.187248	0.183595	0.173716
	$n = 3$	1.54098	1.52845	1.51281	1.47256	0.421882	0.418846	0.414894	0.404335

coincidence of these groups of data are seen. It should be noted that differences percentage in an approximate interval between $p = 0.2$ and $p = 0.6$ are closer to each other than those of other p values for $h/l = 1$, 2 and 3.

This phenomenon represents that in previously mentioned interval, influences of various values of h/l on natural frequency diminishes. It can be discussed that according to Fig. 4 and results of Table 2, due to equivalent differences percentage, for special values of p, natural frequency considering to various values of h/l coincide (as shown in Fig. 4).

The most and the least differences percentage are 0.2041% in $p = 0$ and 0.0289% in $p = 0.6$ for $h/l = 1$, 0.1741% in $p = 0.2$ and 0.0086% in $p = 10$ for $h/l = 2$ and 0.01796% in $p = 0.2$ and 0.0086% in $p = 1.2$ for $h/l = 3$, respectively.

By over viewing Table 2 it is concluded that, the most difference percentage is 0.2041% for $h/l = 1$ and $p = 0$ and the least is 0.0086% for $h/l = 2$ and $p = 10$ and for $h/l = 3$ and $p = 1.2$. Also, Fig. 5 depicts coincidence amount of presented results and those of Ref. (Ansari *et al*. 2013). It is clear that a small increase in p causes natural frequency to

Table 7 Natural frequencies ω_n of the curved FG nano-beam for $b = 2h$ and various values of n, h/l, L/h, α for the case in which $p = 1$

h/l	ω_n	$L/h = 10$				$L/h = 20$			
		$\alpha = \pi/6$	$\alpha = \pi/4$	$\alpha = \pi/3$	$\alpha = \pi/2$	$\alpha = \pi/6$	$\alpha = \pi/4$	$\alpha = \pi/3$	$\alpha = \pi/2$
1	$n = 1$	6.25952	5.89506	5.42976	4.27234	1.60807	1.52008	1.40506	1.11196
	$n = 2$	24.1296	23.6464	23.0444	21.5319	6.50499	6.39815	6.25952	5.89506
	$n = 3$	50.0565	49.437	48.69	46.8605	14.277	14.146	13.9821	13.5611
2	$n = 1$	1.93859	1.82897	1.68797	1.33332	0.493921	0.467173	0.432105	0.342416
	$n = 2$	7.63292	7.49313	7.31843	6.87424	2.01189	1.98005	1.93859	1.82897
	$n = 3$	16.1962	16.02	15.8101	15.2959	4.45976	4.42135	4.37324	4.24926
4	$n = 1$	0.742427	0.701057	0.647611	0.512491	0.188786	0.178627	0.165281	0.131073
	$n = 2$	2.93305	2.88181	2.81738	2.65225	0.769914	0.758005	0.742427	0.701057
	$n = 3$	6.23863	6.17572	6.10048	5.91501	1.70951	1.69539	1.67759	1.63147
8	$n = 1$	0.336678	0.318033	0.293899	0.232753	0.085573	0.080981	0.074943	0.059452
	$n = 2$	1.33021	1.30744	1.27871	1.20478	0.349025	0.343683	0.336678	0.318033
	$n = 3$	2.8275	2.79996	2.7669	2.68504	0.775053	0.768772	0.760834	0.740186
16	$n = 1$	0.163729	0.154679	0.142958	0.113241	0.04161	0.03938	0.036445	0.028915
	$n = 2$	0.646838	0.635837	0.621937	0.586129	0.169716	0.167127	0.163729	0.154679
	$n = 3$	1.37445	1.36121	1.34529	1.30582	0.376868	0.373833	0.369993	0.359992

Table 8 Natural frequencies ω_n of the curved FG nano-beam for $b = 2h$ and various values of n, h/l, L/h, α for the case in which $p = 5$

h/l	ω_n	$L/h = 10$				$L/h = 20$			
		$\alpha = \pi/6$	$\alpha = \pi/4$	$\alpha = \pi/3$	$\alpha = \pi/2$	$\alpha = \pi/6$	$\alpha = \pi/4$	$\alpha = \pi/3$	$\alpha = \pi/2$
1	$n = 1$	4.64571	4.36808	4.01793	3.15551	1.19869	1.13202	1.0455	0.826381
	$n = 2$	17.7868	17.4047	16.9396	15.7951	4.83714	4.75299	4.64571	4.36808
	$n = 3$	36.6609	36.1646	35.582	34.1906	10.5809	10.474	10.3434	10.0159
2	$n = 1$	1.49898	1.41215	1.30172	1.02656	0.383651	0.362584	0.335139	0.26532
	$n = 2$	5.84823	5.7327	5.59148	5.23997	1.55828	1.53229	1.49898	1.41215
	$n = 3$	12.2767	12.1272	11.9535	11.5392	3.43976	3.40726	3.36745	3.26704
4	$n = 1$	0.599482	0.565379	0.521759	0.412399	0.153122	0.144785	0.133894	0.106107
	$n = 2$	2.34448	2.30058	2.24648	2.1105	0.622569	0.612486	0.599482	0.565379
	$n = 3$	4.92499	4.86967	4.80504	4.64955	1.37604	1.36369	1.34843	1.30965
8	$n = 1$	0.277683	0.262003	0.241899	0.191368	0.070892	0.067046	0.062016	0.049166
	$n = 2$	1.08585	1.06598	1.04139	0.979293	0.288254	0.283646	0.277683	0.262003
	$n = 3$	2.27868	2.25403	2.22508	2.15509	0.637137	0.631545	0.624614	0.606918
16	$n = 1$	0.135939	0.12828	0.118453	0.093734	0.034701	0.03282	0.03036	0.024072
	$n = 2$	0.531518	0.521859	0.509889	0.479618	0.141097	0.138849	0.135939	0.12828
	$n = 3$	1.11495	1.10302	1.089	1.05503	0.311861	0.309143	0.30577	0.297146

approach gradually to a constant amount. In continuance, results of accomplished study on the curved FG nano beam have been presented in seven table based on MCST theory together with inclusion of geometrical term $(1 + z / R)$.

Tables 3-9 contain obtained results of investigating influences of forenamed parameters variations on natural frequency. It should be noted that each of the tables has been prepared for a certain value of p. By investigating the results in great details, following points are concluded.

By increasing the opening angle α, corresponding natural frequency decreases, gradually. This converse influence of α on ω_n become more sensible by crossing from $\pi/3$ to $\pi/2$. Increasing of n, h / l and L / h, generally results in reduction of the procedure rate. However, by increasing the parameters this influence will diminish. It is observed that the larger α, the less influence of the parameters, on the rate of procedure. The most import point is that the less values of the parameters, the more dependency of ω_n on variations of α.

Increasing of mode number leads to an increase in ω_n and this effect become more considerable by crossing from $n = 2$ and $n = 3$. It should be said that increasing of h / l and

Table 9 Natural frequencies ω_n of the curved FG nano-beam for $b = 2h$ and various values of n, h/l, L/h, α for the case in which $p = 10$

h/l	ω_n	$L/h = 10$				$L/h = 20$			
		$\alpha = \pi/6$	$\alpha = \pi/4$	$\alpha = \pi/3$	$\alpha = \pi/2$	$\alpha = \pi/6$	$\alpha = \pi/4$	$\alpha = \pi/3$	$\alpha = \pi/2$
1	$n = 1$	4.21065	3.96527	3.65262	2.8755	1.08603	1.02647	0.94872	0.75082
	$n = 2$	16.0526	15.7327	15.3356	14.3402	4.37675	4.30429	4.21065	3.96527
	$n = 3$	32.9307	32.533	32.0554	30.8875	9.55524	9.46668	9.35645	9.07478
2	$n = 1$	1.39136	1.31254	1.21135	0.957172	0.356124	0.336804	0.311507	0.246862
	$n = 2$	5.40034	5.30109	5.17744	4.86396	1.44427	1.42125	1.39136	1.31254
	$n = 3$	11.2654	11.1432	10.998	10.6431	3.18068	3.15298	3.11843	3.02971
4	$n = 1$	0.5688	0.537029	0.496065	0.392652	0.145344	0.137509	0.127228	0.100901
	$n = 2$	2.21212	2.1732	2.12441	1.99976	0.589987	0.580794	0.5688	0.537029
	$n = 3$	4.61469	4.56793	4.51212	4.37483	1.30078	1.2899	1.27625	1.24097
8	$n = 1$	0.266056	0.251273	0.23218	0.183893	0.067961	0.064306	0.059507	0.047207
	$n = 2$	1.03453	1.01664	0.994137	0.936453	0.275885	0.271625	0.266056	0.251273
	$n = 3$	2.15565	2.13442	2.10899	2.0462	0.60826	0.603257	0.596958	0.580636
16	$n = 1$	0.13063	0.123383	0.114018	0.090322	0.033365	0.031572	0.029217	0.02318
	$n = 2$	0.507879	0.499139	0.488136	0.459903	0.135445	0.133359	0.13063	0.123383
	$n = 3$	1.05782	1.04749	1.0351	1.00448	0.298613	0.296169	0.293089	0.285101

L/h cause this procedure to diminish. For instance in larger values of h/l, dependency of ω_n on mode number descends. However, an increase in opening angle leads to an increase in this procedure. This influence shows off more significantly by crossing from $\pi/3$ to $\pi/2$. Generally, it can be said that for larger mode numbers influences of other parameters variations on dependency of ω_n on n diminishes and if α has its possible maximum value and h/l and L/h have their minimum value, variations of n will affect ω_n more significantly.

Converse influence of h/l on ω_n is in such a way that increasing of first parameter result in an exponential reduction of second one, that is variations of h/l for its smaller values are more effective than larger values.

For larger values of α and L/h, rate of this procedure descends, exponentially whit a negative gradient. This effect is more sensible by crossing from $\pi/3$ to $\pi/2$. In addition, an increase in mode number causes sensitivity of natural frequency about variations of h/l to increase. Generally, it can be concluded that for smaller values of α and L/h and larger values of n, dependency of ω_n on variations of h/l is observed more considerably.

In continuance, it is observed that, reduplicating L/h leads to a decrease in ω_n. Increasing of mode number leads to an increase in increment rate of this effect. Also it is observed that this effect, by crossing from $n = 1$ to $n = 2$, is more influent than crossing from $n = 2$ to $n = 3$. It should be expressed that, increasing of h/l and α causes the rate of this procedure to decrease. Increasing of α from $\pi/3$ to $\pi/2$ affects the rate more considerably. Therefore, it can be concluded that, the higher mode number and larger values of h/l and α, the more dependency of ω_n on variations of L/h.

Generally, aforementioned relations and influences may be concluded from each of Tables 3-9. However in order to investigate other influences of parameters on natural frequency, all of the seven tables should be evaluated.

As it is observed in Tables 3-9, an increase in gradient index p leads to reduction of ω_n, gradually. These influences become more sensible in continuance (by increasing of p). However by crossing from $p = 5$ to $p = 10$, dependency of ω_n on p decreases. It should be pointed out that for larger values of h/l, α and L/h, dependency of natural frequency on p diminishes, gradually. Conversely, for larger mode numbers, the dependency rate increases. By overviewing the results, it can be understood that, by increasing of p, influences of h/l, α, L/h and n variations on ω_n, decrease. For all cases by crossing from $p = 5$ to $p = 10$, this converse influence of p diminishes.

5. Conclusions

In free vibration problem of a curved FG nano beam based on modified couple stress theory, natural frequency as a vibration characteristic of the beam has been investigated. Employed beam theory in this study is Timoshenko beam model. In accordance with base relations of MCST theory and utilized beam model, governing equations of motion and related boundary conditions have been derived based on Hamilton's principle. Then in order to solve differential equations Navier's solution method has been adopted and numerical results have been achieved by solving obtained eigenvalue problem, numerically. In continuance, influences of dimensionless length scale parameter h/l, aspect ratio L/h, gradient index p, opening angle α, mode number n and their interactive influences on natural frequency have been investigated and in order to validate the results, some of them have been compared with those of a previous work and differences percentage have been presented. Some important conclusions are as following:

- The main reason of discrepancies between presented

results and those of reference is inclusion of geometrical term $(1 + z / R)$ in this study.

- Increasing of opening angle, increasing of L/h due to slenderizing and lengthening the beam, increasing of ceramic volume fraction due to increasing of gradient index p and ascending of dimensionless length scale parameter h/l, each of them with its particular rate causes natural frequency to decrease. However, conversely, by increasing of mode number natural frequency increases.
- By capturing influence of geometrical term and approaching to a more real condition in theoretical analysis, natural frequency of the curved FG nano beam becomes more sensitive than the case in which geometrical term$(1 + z / R)$ is neglected.
- If geometrical term $(1 + z / R)$ is ignored, results of this paper will be in accord with those of previous works about curved FG nano beams. Furthermore, if radius of curvature is set to infinity, an excellent agreement will be achieved between results of this study and those of previous works about straight FG nano beams.

References

Akgöz, B. and Civalek, Ö. (2013), "Free vibration analysis of axially functionally graded tapered Bernoulli–Euler microbeams based on the modified couple stress theory", *Compos. Struct.*, **98**, 314-322.

Ansari, R., Gholami, R. and Sahmani, S. (2013), "Size-dependent vibration of functionally graded curved microbeams based on the modified strain gradient elasticity theory", *Arch. Appl. Mech.*, **83**(10), 1439-1449.

Arbind, A. and Reddy, J.N. (2013), "Nonlinear analysis of functionally graded microstructure-dependent beams", *Compos. Struct.*, **98**, 272-281.

Asghari, M., Kahrobaiyan, M. and Ahmadian, M. (2010), "A nonlinear Timoshenko beam formulation based on the modified couple stress theory", *Int. J. Eng. Sci.*, **48**(12), 1749-1761.

Chong, A. and Lam, D.C. (1999), "Strain gradient plasticity effect in indentation hardness of polymers", *J. Mater. Res.*, **14**(10), 4103-4110.

Darabi, M., Darvizeh, M. and Darvizeh, A. (2008), "Non-linear analysis of dynamic stability for functionally graded cylindrical shells under periodic axial loading", *Compos. Struct.*, **83**(2), 201-211.

Ebrahimi, F. and Daman, M. (2016), "Dynamic modeling of embedded curved nanobeams incorporating surface effects", *Coupled Syst. Mech., Int. J.*, **5**(3), 255-267.

Ebrahimi, F. and Daman, M. (2017), "Analytical investigation of the surface effects on nonlocal vibration behavior of nanosize curved beams", *Adv. Nano Res., Int. J.*, **5**(1), 35-47.

Fereidoon, A., Andalib, M. and Hemmatian, H. (2015), "Bending Analysis of Curved Sandwich Beams with Functionally Graded Core", *Mech. Adv. Mater. Struct.*, **22**(7), 564-577.

Hajianmaleki, M. and Qatu, M.S. (2012), "Static and vibration analyses of thick, generally laminated deep curved beams with different boundary conditions", *Compos. Part B: Eng.*, **43**(4), 1767-1775.

Hosseini, S. and Rahmani, O. (2016a), "Free vibration of shallow and deep curved FG nanobeam via nonlocal Timoshenko curved beam model", *Appl. Phys. A*, **122**(3), 1-11.

Hosseini, S. and Rahmani, O. (2016b), "Surface effects on buckling of double nanobeam system based on nonlocal Timoshenko model", *Int. J. Struct. Stabil. Dyn.*, **16**(10),1550077.

Hosseini, S.A.H. and Rahmani, O. (2016c), "Thermomechanical vibration of curved functionally graded nanobeam based on nonlocal elasticity", *J. Therm. Stress.*, 1-16.

Jandaghian, A.A. and Rahmani, O. (2015), "On the buckling behavior of piezoelectric nanobeams: An exact solution", *J. Mech. Sci. Technol.*, **29**(8), 3175-3182.

Jandaghian, A.A. and Rahmani, O. (2016), "An Analytical Solution for Free Vibration of Piezoelectric Nanobeams Based on a Nonlocal Elasticity Theory", *J. Mech.*, **32**(2), 143-151.

Jomehzadeh, E., Noori, H. and Saidi, A. (2011), "The size-dependent vibration analysis of micro-plates based on a modified couple stress theory", *Physica E: Low-dimens. Syst. Nanostruct.*, **43**(4), 877-883.

Lam, D., Yang, F., Chong, A., Wang, J. and Tong, P. (2003), "Experiments and theory in strain gradient elasticity", *J. Mech. Phys. Solids*, **51**(8), 1477-1508.

Lanhe, W., Hongjun, W. and Daobin, W. (2007), "Dynamic stability analysis of FGM plates by the moving least squares differential quadrature method", *Compos. Struct.*, **77**(3), 383-394.

Liu, Y. and Reddy, J. (2011), "A nonlocal curved beam model based on a modified couple stress theory", *Int. J. Struct. Stabil. Dyn.*, **11**(3), 495-512.

Ma, H., Gao, X.-L. and Reddy, J. (2008), "A microstructure-dependent Timoshenko beam model based on a modified couple stress theory", *J. Mech. Phys. Solids*, **56**(12), 3379-3391.

Ma, H., Gao, X.-L. and Reddy, J. (2011), "A non-classical Mindlin plate model based on a modified couple stress theory", *Acta Mechanica*, **220**(1-4), 217-235.

McFarland, A.W. and Colton, J.S. (2005), "Role of material microstructure in plate stiffness with relevance to microcantilever sensors", *J. Micromech. Microeng.*, **15**(5), 1060.

Mohammad-Abadi, M. and Daneshmehr, A. (2014), "Size dependent buckling analysis of microbeams based on modified couple stress theory with high order theories and general boundary conditions", *Int. J. Eng. Sci.*, **74**, 1-14.

Nateghi, A., Salamat-talab, M., Rezapour, J. and Daneshian, B. (2012), "Size dependent buckling analysis of functionally graded micro beams based on modified couple stress theory", *Appl. Math. Model.*, **36**(10), 4971-4987.

Nie, G. and Zhong, Z. (2012), "Exact Solutions for Elastoplastic Stress Distribution in Functionally Graded Curved Beams Subjected to Pure Bending", *Mech. Adv. Mater. Struct.*, **19**(6), 474-484.

Park, S. and Gao, X. (2006), "Bernoulli–Euler beam model based on a modified couple stress theory", *J. Micromech. Microeng.*, **16**(11), 2355.

Park, S.K. and Gao, X.L. (2008a), "Micromechanical Modeling of Honeycomb Structures Based on a Modified Couple Stress Theory", *Mech. Adv. Mater. Struct.*, **15**(8), 574-593.

Park, S. and Gao, X.-L. (2008b), "Variational formulation of a modified couple stress theory and its application to a simple shear problem", *Zeitschrift für angewandte Mathematik und Physik*, **59**(5), 904-917.

Qatu, M.S. (2004), *Vibration of Laminated Shells and Plates*, Elsevier.

Rahmani, O., Hosseini, S.A.H. and Hayati, H. (2016), "Frequency analysis of curved nano-sandwich structure based on a nonlocal model", *Modern Phys. Lett. B*, **30**(10), 1650136.

Roque, C., Ferreira, A. and Jorge, R. (2007), "A radial basis function approach for the free vibration analysis of functionally graded plates using a refined theory", *J. Sound Vib.*, **300**(3), 1048-1070.

Salamat-talab, M., Nateghi, A. and Torabi, J. (2012), "Static and dynamic analysis of third-order shear deformation FG micro beam based on modified couple stress theory", *Int. J. Mech. Sci.*, **57**(1), 63-73.

Shafiei, N., Kazemi, M. and Fatahi, L. (2015), "Transverse vibration of rotary tapered microbeam based on modified couple stress theory and generalized differential quadrature element method", *Mech. Adv. Mater. Struct.*, **24**(3), 240-252.

Shariat, B.S. and Eslami, M. (2007), "Buckling of thick functionally graded plates under mechanical and thermal loads", *Compos. Struct.*, **78**(3), 433-439.

Şimşek, M., Kocatürk, T. and Akbaş, Ş.D. (2013), "Static bending of a functionally graded microscale Timoshenko beam based on the modified couple stress theory", *Compos. Struct.*, **95**, 740-747.

Şimşek, M. and Reddy, J. (2013), "Bending and vibration of functionally graded microbeams using a new higher order beam theory and the modified couple stress theory", *Int. J. Eng. Sci.*, **64**, 37-53.

Thai, H.-T. and Choi, D.-H. (2013), "Size-dependent functionally graded Kirchhoff and Mindlin plate models based on a modified couple stress theory", *Compos. Struct.*, **95**, 142-153.

Tsiatas, G.C. (2009), "A new Kirchhoff plate model based on a modified couple stress theory", *Int. J. Solids Struct.*, **46**(13), 2757-2764.

Xia, W., Wang, L. and Yin, L. (2010), "Nonlinear non-classical microscale beams: static bending, postbuckling and free vibration", *Int. J. Eng. Sci.*, **48**(12), 2044-2053.

Yang, F., Chong, A., Lam, D. and Tong, P. (2002), "Couple stress based strain gradient theory for elasticity", *Int. J. Solids Struct.*, **39**(10), 2731-2743.

Zand, M.M. (2012), "The dynamic pull-in instability and snap-through behavior of initially curved microbeams", *Mech. Adv. Mater. Struct.*, **19**(6), 485-491.

CC